



Seismic pounding simulation between Two adjacent Buildings

Sanjeema Bajracharya^a, Uzwal Pokharel^a, Ujwal Katwal^{a,*}, Samir Karki^a, Rajiv Bajgain^a, Umesh Upadhaya^a and Subigya Kumar Yadav^a

^aDepartment of Civil Engineering, IOE Thapathali Campus, Kathamandu, Nepal

ARTICLE INFO

Article history:

Received 5 August 2025
Revised in 7 December 2025
Accepted 23 December 2025

Keywords:

Seismic hazard
Pounding force
Time history analysis
Joint acceleration
Spectral matching

Abstract

The seismic hazard of structures colliding during an earthquake, arising from constrained separation gaps between adjacent buildings, constitutes a significant concern. This phenomenon is particularly pronounced in seismically active region like Kathmandu with dense plinth to land space ratio. Such scenarios result in heightened risks of collisions, increased building displacements with instantaneous acceleration, and greater ductility demands. This research delves into the impact of pounding on adjacent Reinforced Concrete (RCC) buildings aligned and symmetric on plan. The focus is specifically on two neighboring buildings with different storey heights but same floor heights, also designing them using relevant IS codes. The investigation also explores the influence of the initial separation gap between the interacting structures on pounding force. The building models are constructed using ETABS software, and time history analysis is employed for the evaluation and spectral matching is done with SeismoMatch2025. The findings, covering pounding force, joint acceleration before and after pounding are presented and analyzed. The seismic gap provided as per IS 1893: 2016 is sufficient to control seismic pounding and insufficient gap leads to more pounding than no seismic gap.

©JIEE Thapathali Campus, IOE, TU. All rights reserved


1. Introduction

The risk of substantial local damage or potential structural collapse arises when nearby buildings or structures collide during an earthquake. Seismic Pounding emerges as a significant worry when adjoining structures have different natural frequencies, resulting in the occurrence of out of sync vibration. This problem is not limited to buildings and can also arise during the construction of bridges or towers which are situated closely. The concern of seismic pounding becomes particularly crucial in regions susceptible to frequent earthquakes, especially those marked by the dense clustering of multi-story buildings. In location, where seismic pounding conditions are prevalent, it is crucial to examine and mitigate the potential consequences of structures vibrating out of phase. Figure 1 shows the example of seismic pounding.

The occurrence of structural pounding has been observed in various historical earthquakes. Prominent

examples include seismic events such as the 1944 El Centro earthquake, the 1985 Mexico earthquake, the 1994 Northridge earthquake, and the 1995 Kobe earthquake. The 1985 Mexico earthquake [1], in particular, is noteworthy for causing the most extensive reported damages, with around 40% of impacted structures experiencing some degree of pounding and structural collapse. Moreover, 15% of the documented structures were noted to have collapsed entirely. The 1989 Loma Prieta earthquake revealed more than 500 buildings with over 200 instances of pounding, underscoring the widespread occurrence of this phenomenon. Subsequent earthquakes as per Hanks [2], including those in Lorca, Spain (2001), Wenchuan, Sichuan Province in China (2008), Christchurch (2011), and Gorkha, Nepal (2015) [3], also illustrated instances of pounding between neighboring structures. Notably, the Gorkha earthquake featured pounding events in multi-storied Reinforced Concrete (RC) structures in Kathmandu Valley, with masonry structures in hilly urban settlements in Kavrepalanchok and Sindhupalchok districts exhibiting pounding damage as well. Among these seismic events, masonry structures suffered the most consid-

*Corresponding author:

 katwalujwal4@gmail.com (U. Katwal)

erable damage due to pounding, followed by concrete structures.

Building collision, commonly called ‘pounding’, occurs during an earthquake when, due to their different dynamic characteristics, adjacent buildings vibrate out of phase and the at-rest separation is insufficient to accommodate their relative motions. Pounding means an instance of rapid strong pulsation and sometimes, like hammering, repeated heavy blows. Because building separations in urban areas are often insufficient to preclude pounding, there is a need for safe and economical retrofitting methods to reduce structural pounding. In the past, major earthquakes affecting large metropolitan areas have induced severe pounding damage. In some cases, the additional forces generated by the impact interactions have led to collapse building structures. In other cases, the buildings presented minor local damages, but that pounding may be a serious threat to the structures if a stronger earthquake may have induced. In recent years, research has been done to study the pounding phenomenon. Pounding has been included in the list of important areas to be checked during a seismic evaluation, but in general, the engineer does not have much information on how to evaluate the effects of pounding, nor how to reduce them.

Numerous studies have explored the phenomenon of seismic pounding, a critical issue in earthquake-prone urban areas where adjacent buildings with insufficient separation collide due to out-of-phase vibrations. The literature reveals a growing concern about the vulnerability of structures, especially in densely built environments, and highlights a range of analytical and mitigation approaches. Anagnostopoulos [4] introduced collision shear walls as a novel mitigation strategy, while Lin [5] used spectral analysis to assess pounding probabilities based on dynamic characteristics like building frequency and damping. Ehab [6] and Wang [7] investigated the influence of building configurations, torsional behavior, and nonlinearities using finite element and numerical simulations, providing insights into complex dynamic interactions. Khatami [8] advanced the understanding of pounding mechanics by proposing effective impact damping ratio formulations and models for peak pounding force estimation, addressing limitations in existing predictive tools.

Other studies have emphasized retrofitting and mitigation strategies. Jankowski [9] proposed mechanical linking systems between adjacent buildings to synchronize motion and reduce pounding forces, while Namboothiri [10] and Keerthi [11] focused on identifying key structural parameters—such as stiffness, separation distance, and height differences—that exacerbate pounding effects. Mohamed [12] introduced seismic

fragility functions that incorporate pounding effects for non-seismically designed RC buildings, enhancing probabilistic risk assessment models. Collectively, these studies underline the urgent need for both analytical models and practical design guidelines to reduce seismic pounding damage, particularly in retrofitting older structures and designing new buildings in space-constrained urban environments.

Although numerous international studies have explored the phenomenon of seismic pounding, very few have addressed this problem within the Nepalese context using IS 1893–based spectral matching and local soil conditions. Existing research generally focuses on generic pounding scenarios, without integrating code-specific provisions or performance-based evaluation for densely built regions like Kathmandu Valley. This study bridges that gap by conducting nonlinear time-history analysis of adjacent reinforced concrete moment-resisting frame (RCMRF) buildings designed according to IS 456:2000 and IS 1893:2016. Seven real earthquake ground motions, spectrally matched to the IS design spectrum using SeismoMatch2025, are employed to replicate Nepal’s seismic environment. The study contributes by: (i) evaluating pounding sensitivity across varying seismic gaps (0–100 mm); (ii) identifying an empirical threshold gap that effectively prevents impact; and (iii) comparing this threshold with the conservative IS 1893:2016 code-prescribed gap. The results offer practical implications for optimizing building spacing in dense urban areas of Nepal while maintaining seismic safety.

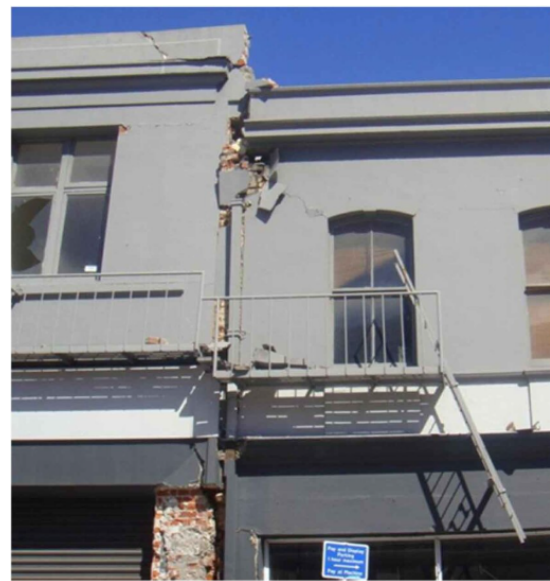


Figure 1: Pounding Damage observed in ChristChurch 2011 [13]

2. Numerical simulation

For the non-linear dynamic analysis of seismic pounding between adjacent buildings, seven real earthquake ground motions were selected as input excitations from the Pacific Earthquake Engineering Research (PEER) NGA database [14] to ensure realistic and diverse seismic loading. These motions represent moderate to large earthquakes recorded on soft to medium-soft soil sites, consistent with Kathmandu Valley conditions. The selected records and their key parameters are listed in Table 1. Further details on the selection criteria, spectral matching, and scaling procedure are provided in the following paragraph.

The seven earthquake ground motions were obtained from the Pacific Earthquake Engineering Research (PEER) NGA database, selected to represent a wide range of magnitudes (6.5 – 7.6), distances, and site conditions typical of the Kathmandu Valley. The key selection criteria included: (i) availability of horizontal components with well-documented metadata; (ii) soft to medium-soft soil conditions corresponding to V_{s30} values between 120 m/s and 200 m/s (Site Class D/E as per IS 1893:2016); and (iii) strong-motion duration and spectral shape comparable to those expected in the design seismic zone of Nepal (Zone V).

Each record was spectrally matched to the IS 1893:2016 design response spectrum using SeismoMatch 2025. The matching was performed in the frequency range of 0.1 – 5.0 s, covering the fundamental periods of both buildings (0.6 – 1.0 s). Peak ground accelerations (PGA) of the matched records were scaled to approximately 0.36 g, corresponding to the Zone V design intensity for the Kathmandu region. For validation, spectral acceleration (S_a), peak ground velocity (PGV), and predominant period (T_p) of the adjusted records were compared to confirm consistency with the target design spectrum. Figure 2 and Figure 3 present the spectral matching results before and after adjustment, demonstrating close conformity to the IS 1893:2016 target spectrum.

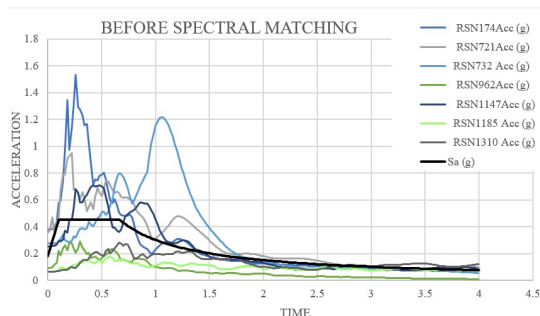


Figure 2: Before spectral matching

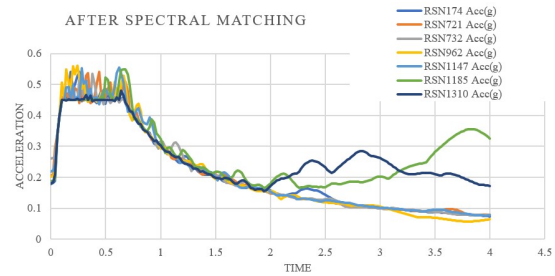


Figure 3: After spectral matching

The selected ground motion records summarized in Table 1 and spectrally matched as shown in figure 2 and 3 above represent a realistic set of input excitations for seismic pounding analysis. They cover a broad range of moderate to large earthquake magnitudes (6.5 to 7.6) and include recordings from diverse tectonic regions such as California, Turkey, and Taiwan. This diversity introduces variability in fault mechanisms and frequency content, which is essential for assessing the robustness of the pounding response. The V_{s30} values, ranging from approximately 124 to 198 m/s, correspond to soft to medium-soft soil conditions (Site Class D/E), typical of dense urban areas such as the Kathmandu Valley. These soil profiles are known to amplify ground motion, making them particularly suitable for studying seismic pounding effects in space-constrained urban environments.

3. Structural and seismic design of building

To investigate seismic pounding between adjacent buildings, two reinforced concrete (RC) moment-resisting frame structures were selected with differing heights to simulate varied dynamic behavior under seismic loading. A six-storey and a three-storey building were modeled, both with consistent inter-storey heights of 3.0 meters and identical plan dimensions. Each building has a 3×3 bay configuration with 4-meter spans in both directions, resulting in a square footprint of 12 m × 12 m as shown in Figure 4. This setup enables the analysis of vertical geometric irregularity, a critical factor influencing inter-structural pounding.

The buildings are assumed to be located in Kathmandu Valley, a high seismic zone characterized by soft soil conditions. Structural design was performed in compliance with Indian Standards—IS 456:2000 for RC detailing and IS 1893:2016 for seismic loading. Dead and live loads were considered as per IS 875 Parts 1 and 2. The floor finish was modeled as 1 kN/m², while live loads were taken as 2 kN/m² for typical floors and 1.5 kN/m² for the roof. Wall loads were calculated as-

Table 1: Selected Ground Motion from the PEER NGA database used for spectral matching to the IS 1893:2016 design spectrum

Year	Symbol	Earthquake Name	Station	Magnitude	Vs30 (m/s)
1979	RSN174	Imperial Valley-06	El Centro Array #11	6.53	196.25
1987	RSN721	Superstition Hills-02	El Centro Imp. Co. Cent	6.54	192.05
1989	RSN732	Loma Prieta	APEEL 2 - Redwood City	6.93	133.11
1994	RSN962	Northridge-01	Carson - Water St	6.69	160.58
1999	RSN114	Kocaeli, Turkey	Ambarli	7.51	175
1999	RSN118	Chi-Chi, Taiwan	CHY012	7.62	198.4
1999	RSN131	Chi-Chi, Taiwan	ILA004	7.62	124.27

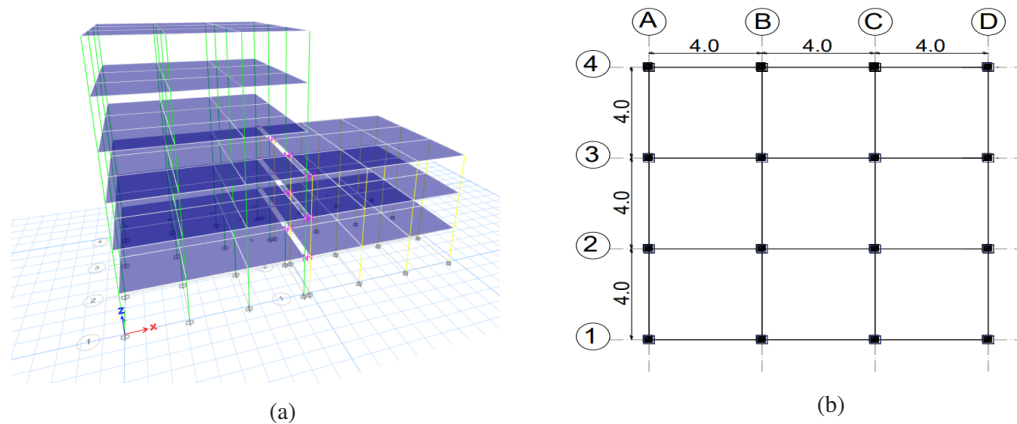


Figure 4: One six storey and one storey building with same floor plan (a) Elevation (b) Plan

suming a unit weight of 20 kN/m^3 , with a 30% opening deduction for external walls.

Preliminary design was conducted to satisfy strength and serviceability limits. Effective depths and cross-sectional dimensions for slabs, beams, and columns were determined using deflection control criteria. Slabs were designed as two-way slabs, while beams and columns were sized based on ultimate moment and axial capacity checks, incorporating partial safety factors and appropriate reinforcement percentages. Reinforced concrete grades of M25 for columns and M20 for beams were used, along with Fe500 grade steel.

This building configuration facilitates a focused study on pounding behavior due to height difference while minimizing plan irregularities. It forms the basis for time history analysis and evaluation of inter-structural impact under real earthquake ground motions.

3.1. Building Finite Element Modelling

To assess the seismic pounding effects between adjacent structures of unequal height, detailed three-dimensional (3D) finite element (FE) models were developed using ETABS 2016. The selected structures consist of

a 3-storey and a 6-storey reinforced concrete moment-resisting frame (RCMRF) building. Each building has a regular plan geometry measuring $12 \text{ m} \times 12 \text{ m}$, with three bays in both the X and Y directions, each 4 meters wide. A uniform inter-storey height of 3.0 meters was maintained across both buildings, reflecting typical mid-rise urban construction in seismic-prone regions such as the Kathmandu Valley.

The modeling process adhered to the Indian Standards for design and loading: IS 456:2000 for reinforced concrete structural design, and IS 1893:2016 for earthquake-resistant design of structures. The buildings were modeled using M25 grade concrete for columns and M20 for beams, with Fe500 grade steel reinforcement. Dead load was computed based on self-weight and wall loads, assuming a unit weight of 20 kN/m^3 with 30% opening deduction in the outer walls. Live loads of 2.0 kN/m^2 for intermediate floors and 1.5 kN/m^2 for the roof were considered, in line with IS 875 (Part 2). Slab weights were transferred to beams using yield line theory.

Masonry infill walls were not included in the analytical model because, in reinforced concrete moment-resisting

frames (RC-MRF), infills are generally not considered structural elements and are typically excluded from lateral load-resisting calculations in standard engineering practice. Following this convention, the present study modeled the buildings as bare frames. This approach allows the analysis to focus specifically on frame-to-frame interaction without introducing additional uncertainties related to nonstructural components. The implication of this assumption has been acknowledged in the Discussion and Conclusion sections.

3.2. Structural impact model

To simulate the collision behavior between adjacent buildings during seismic events, a structural impact model was incorporated into the finite element framework. The pounding phenomenon is addressed through a simplified yet effective approach by introducing a linear elastic contact element that becomes active only when the separation gap between the buildings is closed during lateral vibration.

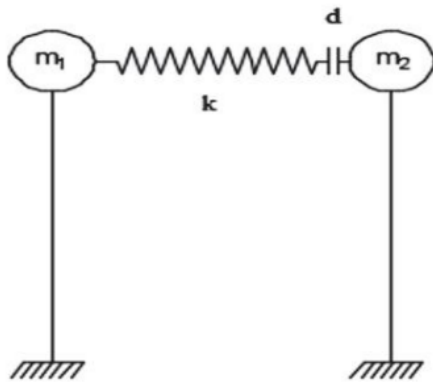


Figure 5: Contact or Link element

In the ETABS model, pounding between the two buildings was simulated using compression-only gap/link elements placed at each corresponding floor level. These elements remain inactive while the separation between the buildings is greater than the assigned gap, and become active only when the relative displacement closes the gap. When activated, the link behaves as a uniaxial nonlinear compression-only spring. In this study, the contact law is simplified as a linear elastic impact model, where the impact force is proportional to the interpenetration depth. This is mathematically expressed in the equation below. No tensile force is allowed, and no contact is generated unless the buildings physically touch. The stiffness k was estimated based on the axial stiffness of the colliding structural components and refined using formulations available in Polycarpou [15]. This approach enables effective simulation of pounding within ETABS while maintaining numerical stability.

This mechanism is schematically illustrated in Figure 5, showing the interaction between adjacent masses connected by an elastic spring element.

The pounding force $F(t)$ generated by this contact spring is mathematically expressed as:

$$F(t) = \begin{cases} k \delta(t), & x \geq 0 \\ 0, & x < 0 \end{cases} \quad (1)$$

$$\delta(t) = u_1(t) - u_2(t) - d \quad (2)$$

where k is the stiffness of the spring, $\delta(t)$ is the interpenetration depth (i.e., the amount by which the gap is closed), $u_1(t)$ and $u_2(t)$ are the absolute displacements of the two adjacent buildings at time t , and d is the initial gap or separation distance.

It is important to acknowledge that the adopted impact model is purely linear elastic, meaning that no hysteretic energy loss, damping, or permanent deformation is included during impact. In reality, pounding is a highly nonlinear phenomenon involving localized crushing of concrete, friction, impact damping, and possibly inelastic deformation. The linear elastic assumption therefore provides a conservative estimate of peak pounding forces, as it does not account for any energy dissipation during collision. This limitation is recognized and discussed in the Conclusion section as an area for future improvement.

To calculate the impact stiffness coefficient (k), several approaches can be adopted. The most basic formula estimates the stiffness based on axial deformation properties of the colliding structural elements, given by:

$$k = \frac{EA}{L} \quad (3)$$

where E is the modulus of elasticity of concrete, A is the cross-sectional area of the contact surface (typically the beam or slab edge), and L is the length over which deformation occurs (typically the beam span or contact length).

However, more refined expressions have been developed to improve realism in modeling contact behavior. For instance, Polycarpou [15] proposed a modified expression for the normal direction stiffness of the contact interface:

$$k = \frac{4E_{\text{DYN}}\sqrt{R}}{3(1-\nu^2)} \quad (4)$$

where ν is Poisson's ratio, taken as 0.2 for concrete, E_{DYN} is the dynamic modulus of elasticity, given by

$$E_{DYN} = 5.82 (E_{STATIC})^{0.63} \text{ GPa,}$$

and E_{STATIC} is the static modulus of elasticity, given by

$$E_{STATIC} = 5000\sqrt{f_{ck}}.$$

4. Code specified separation to avoid pounding

One of the critical safety considerations in the seismic design of adjacent buildings is the provision of adequate separation distance to prevent structural pounding. Pounding occurs when buildings, having different dynamic characteristics such as height, stiffness, or mass distribution, move out of phase during an earthquake and collide. To address this risk, several international and national design codes have established guidelines or mandatory provisions for minimum separation distances between adjacent buildings or structural units. These provisions are typically based on expected seismic displacements, ensuring that even under extreme lateral motion, structures remain free from unintended contact.

The Indian Standards provide some of the clearest and most direct instructions on this issue. According to IS 4326, Clause 5.1 mandates that separation be provided between adjoining structures or parts of the same structure if they differ in total height, storey height, or dynamic response. The underlying rationale is to allow independent lateral movement of structures under seismic loading without the risk of collision. The code provides minimum gap width recommendations graphically in Figure 2.6 and specifies that the seismic coefficient used in these calculations should align with IS 1893:1984. IS 1893 (Part 4):2015 further refines this approach in Clause 11.2 by stating that the separation distance should be equal to the product of the response reduction factor (R) and the sum of maximum storey displacements of the adjacent structures. This formula ensures that the calculated separation is responsive to the structural system, ductility, and expected performance level of each building. Specifically, if two structures deflect toward each other during seismic shaking, the minimum gap must satisfy:

$$\text{Gap distance} \geq R(\delta_1 + \delta_2) \quad (5)$$

where δ_1 and δ_2 are the maximum calculated displacements of the respective buildings.

The Nepal National Building Code NBC 105:2020, which governs seismic design within the Federal Democratic Republic of Nepal, broadly aligns with this philosophy, although it does not specify a formula for pounding separation. Instead, it offers a comprehensive framework for the seismic design of buildings made from reinforced concrete, steel, composite materials, timber, and masonry, and expects designers to prevent pounding by ensuring seismic displacements are appropriately managed. The code emphasizes performance-based analysis and appropriate detailing rather than prescribing fixed gap values, thereby giving engineers flexibility within a rigorous safety-first approach.

This philosophy of displacement-based separation is also echoed in global design codes. The International Building Code (IBC), although it does not mention pounding explicitly, indirectly addresses it through its provisions on seismic design categories and structural drift limits. For adjacent buildings of similar height and alignment, IBC requires that the expected seismic drift be used to compute minimum separations. Similarly, Eurocode 8 (EN 1998-1), which is widely adopted across Europe, requires that buildings be separated by at least the sum of their peak lateral displacements under design-level ground motions. Although EC8 does not explicitly use the term "pounding," its requirements on drift control and seismic separation distances imply a direct concern with avoiding structural collisions during earthquakes.

To better understand the similarities and differences in how these codes address seismic pounding, the following Table 2 summarizes the key provisions of each:

In the United States, ASCE 7-22 offers clear guidance on this topic. It recommends that the minimum separation distance between adjacent structures be equal to the sum of their maximum inelastic displacements under design-level ground motion. This is conceptually identical to the IS 1893 formulation, although it is expressed in drift-based terms rather than through a response reduction factor. The NEHRP guidelines further support this approach by providing general recommendations for building configuration and seismic detailing practices that implicitly mitigate pounding risk. While NEHRP does not provide a direct formula for separation, it emphasizes dynamic interaction modeling, proper energy dissipation, and redundancy in structural systems.

In comparing these diverse codes, a consistent principle emerges: the required separation between buildings must be based on their relative displacement capacity under seismic excitation. The methodologies

Table 2: Design Codes and their Provisions related to Seismic Pounding

Design Code / Standard	Relevant Provisions
IS 4326	Clause 5.1 mandates separation between adjoining structures with different heights or dynamic properties to prevent pounding. Seismic coefficient as per IS 1893:1984.
IS 1893 (Part 4)	Clause 11.2 recommends a separation distance $\geq R(\delta_1 + \delta_2)$, where R is the response reduction factor and δ_1, δ_2 are maximum storey displacements of the two structures.
NBC 105:2020 (Nepal Building Code)	Applies to all building types in Nepal. Covers seismic design and analysis for RC, steel, timber, and masonry buildings. Though not specific on pounding, it sets the national framework for seismic safety.
International Building Code (IBC)	Provides seismic design categories and requirements for force-resisting systems. Does not explicitly mention pounding, but addresses building separation and structural detailing that mitigate collision risk.
Eurocode 8 (EC8)	Offers comprehensive seismic design parameters and analysis methods for European structures. While seismic pounding is not directly specified, EC8 indirectly addresses building separation requirements.
ASCE 7-22	Covers minimum design loads and criteria for seismic design in the U.S. Though pounding is not specifically named, it includes rules on separation distance, detailing, and dynamic interaction.
NEHRP Guidelines	Recommends earthquake-resistant practices, including configuration and dynamic response considerations. While it doesn't explicitly address pounding, it emphasizes detailing and modeling to mitigate its effects.

vary slightly—some are tabular (IS 4326), some formulaic (IS 1893, ASCE 7), and others performance-based (NBC 105, EC8)—but the goal remains the same: to ensure that buildings can deform safely without interacting destructively with their neighbors.

5. Analysis

To examine the effects of seismic pounding between adjacent structures with varying dynamic characteristics, a pair of reinforced concrete moment-resisting frame (RCMRF) buildings with different storey heights—specifically, one with three storeys and another with six storeys—was selected for the study. These two buildings were aligned adjacently with uniform floor heights and identical bay widths, creating a realistic scenario that commonly occurs in dense urban settings. Due to the difference in structural height and stiffness, the buildings exhibit different fundamental vibration periods, which increases the likelihood of out-of-phase movement and collision during seismic excitation. To simulate and analyze the influence of separation distance on pounding behavior, a total of seven

pounding cases were modeled by varying the seismic gap between the two buildings. The selected separation gap values were 0 mm, 5 mm, 15 mm, 25 mm, 50 mm, and 100 mm, enabling a thorough investigation of scenarios ranging from no separation (direct contact) to generous spacing. These values were deliberately chosen to include both non-compliant gaps (less than code-recommended), compliant gaps (approximately 25 mm), and larger-than-required gaps to assess how sensitive the building responses are to increasing clearance. Each configuration was subjected to seven distinct ground motion records representing moderate to strong earthquakes with varying frequency content and duration, allowing for realistic simulation of seismic impacts. The dynamic analysis was carried out using ETABS, incorporating nonlinear time history analysis and employing contact (gap) elements that remain inactive until the relative displacement between corresponding floor levels exceeds the preassigned separation gap. Once contact occurs, these gap elements activate and transfer compressive impact forces based on linear elastic spring behavior. Structural responses were recorded along the x-direction—corresponding to the adjacent

building alignment—with specific attention given to displacement, inter-storey drift, base shear, and impact forces observed at the building corners, where pounding is most critical. The full schematic of the building configurations and pounding case setup is shown in Figure 6, which illustrates the elevation view and alignment of the two structures with respect to the contact interface and variation in gap widths.

6. Results and discussion

6.1. Modal Characteristics and Influence on Pounding

Before performing the pounding simulations, the numerical models were validated to ensure that the dynamic properties of both buildings were consistent with code expectations and realistic for reinforced concrete moment-resisting frames. The fundamental periods obtained from ETABS were compared with the approximate empirical expression recommended by IS 1893:2016 (Clause 7.6.1)

$$T = 0.075 h^{0.75} \quad (6)$$

where h is the building height in meters. For the 6-storey (18 m) and 3-storey (9 m) buildings, the code-based estimates were approximately 1.02 s and 0.58 s, respectively. The ETABS-computed periods as shown in Table 3 showed deviations within 5%, confirming that the global stiffness of both numerical models is consistent with IS 1893 expectations. Additionally, maximum elastic roof displacements from the equivalent static method differed by less than 8% from those obtained from the response spectrum analysis. This close agreement indicates adequate numerical stability and validates the models for subsequent time-history analysis and pounding simulation.

Following validation, the modal characteristics of the two buildings were examined to understand their influence on the likelihood and severity of seismic pounding. Modal analysis revealed distinct differences in the dynamic properties of the structures due to their height and stiffness variation. The fundamental periods of the 6-storey building were found to be 1.034 s, 1.034 s, and 0.901 s for the first three modes, whereas the 3-storey building exhibited significantly shorter periods of 0.618 s, 0.618 s, and 0.603 s, as summarized in Table 3. These differences indicate that the two buildings possess markedly different natural frequencies, which increases the probability of out-of-phase motion during seismic excitation.

This mismatch in modal properties is a primary cause of pounding. When two adjacent buildings vibrate at

different frequencies, their lateral displacements may peak at different times, resulting in large relative movements even when their absolute displacements are moderate. Under such conditions, insufficient separation gap leads to repeated collisions. Conversely, structures with closely spaced natural periods tend to move more synchronously, reducing the relative displacement and lowering the risk of impact.

Furthermore, resonance effects can amplify the response of a building if its natural period coincides with the dominant period of the input ground motion. For the present configuration, the 6-storey building—with its longer period—is more sensitive to long-period components, while the 3-storey building responds more strongly to short-period content. This dynamic incompatibility becomes particularly critical during multi-frequency seismic excitations, where both buildings may experience peak responses at different times, thereby intensifying the potential for pounding if the separation gap is insufficient.

Table 3: Time period of three modes of each building

Number of Storey	Mode 1	Mode 2	Mode 3
6	1.034 s	1.034 s	0.901 s
3	0.618 s	0.618 s	0.603 s

When buildings vibrate at different frequencies, the relative motion between their floor levels increases during seismic excitation, raising the likelihood of collisions. Conversely, buildings with closely aligned time periods tend to move synchronously, reducing the risk of pounding. Additionally, resonance can amplify building responses when a structure's fundamental frequency aligns with the dominant frequency of ground motion, further escalating the pounding potential if the separation gap is inadequate.

6.2. Seismic gap and code-based requirements

To evaluate separation requirements, the equivalent static method was used per IS 1893:2016, which recommends calculating the minimum gap based on maximum deflections and a response reduction factor. Table 4 shows the resulting values: a maximum displacement of 35.96 mm for the 6-storey building and 15.35 mm for the 3-storey building. Using a response reduction factor $R=5$ (for Special Moment Resisting Frames), the total required gap as per the formula is 256.55 mm. This value serves as a conservative benchmark, ensuring that even the worst-case relative displacements are accommodated.

Seismic pounding simulation between Two adjacent Buildings

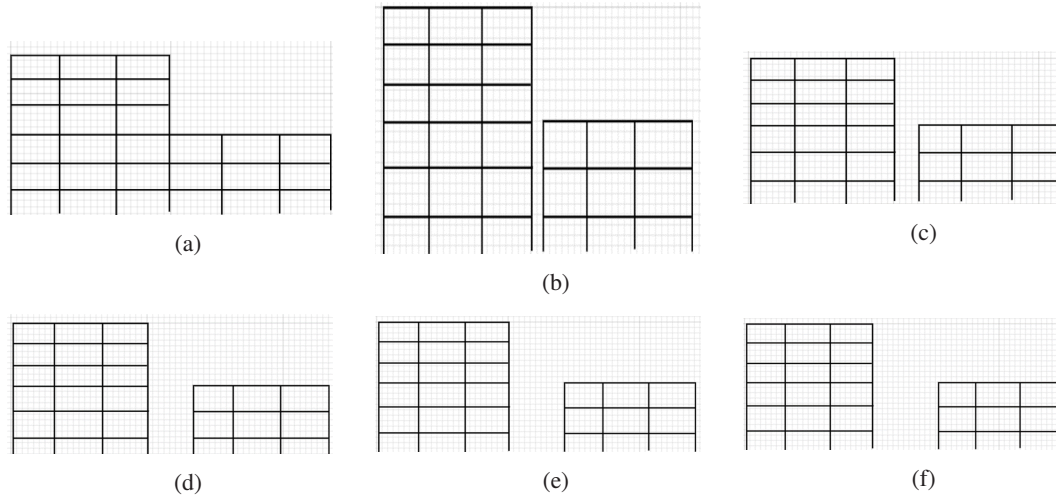


Figure 6: Configuration of Adjacent Buildings (a) 0 mm gap (b) 5 mm gap (c) 15 mm gap (d) 25 mm gap (e) 50 mm gap (f) 100 mm gap

Table 4: Maximum Deflection for SMRF

6 Storey	3 Storey	Maximum Deflection (A)	Maximum Deflection (B)	IS code [R(A+B)]	R=5 For SMRF
A	B	35.96	15.35	256.55	–

6.3. Impact forces from time history analysis

The peak impact forces generated between the two buildings during seismic excitation were evaluated for separation gaps of 0, 5, 15, 25, 50, and 100 mm. The results from the seven selected ground motions are summarized in Table 5. A wide variation in impact force is observed across different earthquakes, reflecting the dependence of pounding on both building-specific dynamic characteristics and the input ground-motion frequency content, duration, and amplitude. This variability underscores the complexity of the pounding phenomenon and the importance of considering multiple earthquakes rather than relying on a single representative record.

To visualize the overall trend, Figure 7 presents the mean pounding force across all earthquakes for each separation gap. As expected, the smallest gaps produce the highest impact forces. A gap of 0 mm represents rigid contact, leading to almost instantaneous impact whenever relative motion occurs. Even a 5 mm gap provides minimal free vibration space, causing high relative velocity at the instant of collision, thereby generating large forces.

As the gap increases to 15–25 mm, a notable reduction in pounding force is observed. At these intermediate gaps, the buildings have limited but meaningful clearance to vibrate independently before impact occurs.

This reduces the relative velocity of the buildings at the moment of impact for many earthquakes. However, substantial irregularities remain—certain ground motions continue to produce unexpectedly high forces even at these moderate gaps.

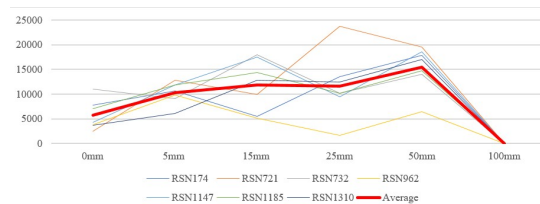


Figure 7: Pounding force(kN)

The non-monotonic and irregular nature of the pounding-force trend is primarily governed by the dynamic interaction and relative acceleration between the two buildings. Because the structures have significantly different natural periods, they respond out of phase during seismic excitation. When their acceleration peaks occur simultaneously, the relative acceleration at the moment of contact becomes large, resulting in higher impact forces if the separation gap is insufficient. Conversely, when the acceleration peaks are misaligned, the differential inertial demand is smaller, reducing the severity of the impact even when displacement overlap occurs.

Table 5: Pounding Force for Building Cases with Different Seismic Separation when taller building is on left

Earthquake Name	No gap kN	5 mm gap kN	15 mm kN	25 mm kN	50 mm kN	100 mm kN
Imperial Valley-06	7742.49	10713	5488.05	13499	17829	0
Superstition Hills-02	2553.51	12802	9892.49	23783	19574	0
Loma Prieta	11058	9050.9	17957	10224	14078	0
Northridge-01	3854.3	9800.47	5101.7	1691.92	6467.5	0
Kocaeli, Turkey	4272.06	11862	17469	9419.93	18551	0
Chi-Chi, Taiwan	7100.33	11917	14328	10214	14776	0
Chi-Chi, Taiwan	3660.33	6092.9	12801	12427	17012	0

At moderate gaps, the intensity of pounding depends strongly on the instantaneous phase relationship between the two buildings at the time of collision. For certain ground motions, such as Hachinohe or Duzce, the taller building develops amplified acceleration demands due to resonance effects associated with long-period components of the input motion. In such cases, the relative acceleration remains large even when gaps exceed 25–50 mm, producing higher impact forces than expected. This explains why increasing the gap does not always lead to a proportional reduction in impact intensity.

Even at a 50 mm gap, some earthquakes still generate notable impact forces, indicating that gap size alone does not control pounding severity—rather, the combination of displacement overlap and relative acceleration dictates the impact outcome. Only at a separation gap of 100 mm does pounding cease for all considered ground motions, confirming that this value is sufficient to prevent both displacements overlap and acceleration-induced collision for the studied configuration.

These observations highlight several engineering implications. First, the occurrence of pounding is triggered by relative displacement overlap, but the severity of pounding is governed by the relative acceleration between adjacent buildings. Second, the non-linear variation in impact forces demonstrates that separation-gap design should not rely on linear scaling or simplified assumptions. Third, because different earthquakes emphasize different frequency components, evaluating pounding performance using multiple ground motions is essential to capture the full range of possible phase-interaction effects.

Overall, the results confirm that a 100 mm seismic separation gap is sufficient to eliminate pounding between the selected 3-storey and 6-storey buildings under the considered ground motions. This gap provides adequate clearance to prevent contact under all evaluated dynamic conditions, making it a practical and conser-

vative recommendation for similar mid-rise building configurations in dense urban environments.

6.4. Code provisions vs. Empirical outcomes

The IS 1893:2016 guideline suggests a minimum separation of 256.55 mm, which is more than double the empirically validated 100 mm. While this difference reflects the conservative nature of code-based design, it also raises questions about efficiency, especially in urban environments where land use optimization is a concern. The simulation results clearly demonstrate that a 100 mm gap is sufficient to eliminate pounding for the given structural configuration and ground motions. Thus, the code's conservative estimate, while safe, may lead to unnecessary spatial and economic inefficiency in practice.

7. Conclusion

This study investigated seismic pounding between two adjacent reinforced concrete moment-resisting frame (RCMRF) buildings of unequal height—a 6-storey and a 3-storey structure—representative of typical mid-rise construction in dense urban areas such as Kathmandu Valley. Both buildings were designed in accordance with IS 456:2000 and IS 1893:2016, and were modeled using ETABS with compression-only contact elements to simulate impact. Seven recorded ground motions from the PEER database, selected for soft to medium-soft soil conditions and spectrally matched to the IS 1893:2016 design spectrum using Seismo-Match 2025, were applied to capture realistic seismic demands.

Modal analysis and model validation showed that the numerically obtained fundamental periods of the buildings closely matched IS 1893:2016 empirical estimates, confirming that the global stiffness representation is realistic. The pronounced difference between the fundamental periods of the two buildings (approximately

1.03 s for the 6-storey and 0.62 s for the 3-storey structure) demonstrated a strong potential for out-of-phase vibration and significant relative displacement, which is a primary driver of pounding.

The nonlinear time-history analyses revealed that when no separation gap or only very small gaps (0–5 mm) were provided, the resulting pounding forces were extremely high, often exceeding 10,000 kN for certain ground motions. These small gaps did not mitigate impact; instead, they intensified it by allowing the structures to develop high relative velocity at the instant of collision. As the gap was increased to intermediate values (15–25 mm), the magnitude of pounding forces generally decreased, but the variation was non-monotonic and strongly dependent on the input motion. Some earthquake records still produced large impact forces even at 50 mm separation, highlighting the importance of dynamic phasing and resonance effects rather than gap size alone. Only at a 100 mm separation gap did pounding forces reduce to zero for all seven ground motions, indicating that this value is sufficient to eliminate impact for the studied configuration.

A key outcome of this study is the comparison between the performance-based empirical gap and the code-prescribed separation distance. The equivalent static analysis as per IS 1893:2016 yielded a recommended separation of approximately 256.55 mm for the pair of buildings considered. By contrast, the dynamic analyses demonstrated that a much smaller gap of 100 mm was adequate to prevent pounding under the selected spectrally matched ground motions. This confirms that the code provisions are intentionally conservative, providing a significant safety margin, but also suggests that performance-based approaches can justify reduced gaps in space-constrained urban environments, provided detailed dynamic assessment is carried out.

From a practical perspective, the results are particularly relevant for urban regions like Kathmandu Valley, where limited land availability and narrow plot widths make large separation gaps difficult to implement. The finding that a 100 mm gap is impact-free for the specific 3-storey and 6-storey RCMRF buildings considered offers a useful benchmark for similar mid-rise building pairs with comparable dynamic characteristics and soil conditions. However, it is emphasized that this value should not be generalized blindly, as pounding behavior is highly sensitive to building stiffness, mass distribution, height ratio, and ground-motion characteristics.

This study has several limitations that also point toward future research needs. The impact model adopted herein is linear elastic and does not explicitly account for energy dissipation, local damage, or nonlinear con-

tact behavior, which may influence detailed impact histories. Masonry infill walls were neglected to isolate frame-to-frame interaction, even though infills can substantially alter stiffness, mass, and damping properties. Furthermore, only planar (2D) pounding along one direction was considered, whereas real structures may experience three-dimensional interaction and torsional effects during earthquakes. Future work should therefore incorporate more refined nonlinear impact models (including impact damping and local damage), consider infill–frame interaction, and extend the analysis to three-dimensional configurations and irregular building layouts. Incorporating a larger suite of ground motions and probabilistic assessment frameworks would also help to develop more robust fragility-based recommendations.

Despite these limitations, the study contributes to the limited body of Nepal-focused pounding research by combining IS 1893:2016–based spectral matching, detailed nonlinear time-history analysis, and explicit evaluation of minimum separation gaps for typical mid-rise RC buildings. The results underline the need to consider dynamic interaction effects in design, and they support the use of performance-based assessment as a complement to codal prescriptions for optimizing building separations in dense urban environments.

References

- [1] Degg M R. Earthquake hazard assessment after Mexico (1985)[M]. 1989.
- [2] Hanks T C, Krawinkler H. Bulletin of the seismological society of America[J]. 1991.
- [3] Shrestha B, Hao H. Building pounding damages observed during the 2015 gorkha earthquake[J/OL]. Journal of Performance of Constructed Facilities, 2018, 32. DOI: [10.1061/\(ASCE\)CF.1943-5509.0001134](https://doi.org/10.1061/(ASCE)CF.1943-5509.0001134).
- [4] Anagnostopoulos S A, Karamaneas C E. Collision shear walls to mitigate seismic pounding of adjacent buildings[R]. 2008.
- [5] Lin J H, Chiang Weng C. Spectral analysis on pounding probability of adjacent buildings[J]. 2001, 23.
- [6] Ehab M, Salem H, Mostafa H, et al. Earthquake pounding effect on adjacent reinforced concrete buildings[J]. 2014, 106.
- [7] Wang L X, Chau K T, Wei X X. Numerical simulations of nonlinear seismic torsional pounding between two single-story structures[J]. 2009.
- [8] Khatami S M, Naderpour H, Barros R C, et al. Effective formula for impact damping ratio for simulation of earthquake-induced structural pounding[J/OL]. Geosciences (Switzerland), 2019, 9. DOI: [10.3390/geosciences9080347](https://doi.org/10.3390/geosciences9080347).
- [9] Jankowski R, Mahmoud S. Linking of adjacent three-storey buildings for mitigation of structural pounding during earthquakes[J/OL]. Bulletin of Earthquake Engineering, 2016, 14: 3075-3097. DOI: [10.1007/s10518-016-9946-z](https://doi.org/10.1007/s10518-016-9946-z).
- [10] Namboothiri V P. Seismic pounding of adjacent buildings[R]. 2017.
- [11] Keerthi R, Prabhakara H R, Ravi Kumar C M, et al. Seismic pounding effect between adjacent buildings[J]. 2015, 3.
- [12] Mohamed H, Romão X. Seismic fragility functions for non-seismically designed rc structures considering pound-

- ing effects[J/OL]. Buildings, 2021, 11. DOI: [10.3390/buildings11120665](https://doi.org/10.3390/buildings11120665).
- [13] Noman M, Alam B, Fahad M, et al. Effects of pounding on adjacent buildings of varying heights during earthquake in pakistan[J/OL]. Cogent Engineering, 2016, 3. DOI: [10.1080/23311916.2016.1225878](https://doi.org/10.1080/23311916.2016.1225878).
- [14] Pacific earthquake engineering research center, new spectra[R]. 2025.
- [15] Polycarpou P C, Papaloizou L, Komodromos P. An efficient methodology for simulating earthquake-induced 3d pounding of buildings[J/OL]. Earthquake Engineering & Structural Dynamics, 2014, 43: 985-1003. DOI: [10.1002/eqe.2383](https://doi.org/10.1002/eqe.2383).